Accepted Manuscript

Synthesis and biological evaluation of α-santonin derivatives as anti-hepatoma agents

Hao Chen, Xiao Yang, Zongmin Yu, Ziying Cheng, Hu Yuan, Zeng Zhao, Guozhen Wu, Ning Xie, Xing Yuan, Qingyan Sun, Weidong Zhang

PII: S0223-5234(18)30210-1

DOI: 10.1016/j.ejmech.2018.02.073

Reference: EJMECH 10250

To appear in: *European Journal of Medicinal Chemistry*

Received Date: 11 October 2017

Revised Date: 5 February 2018

Accepted Date: 21 February 2018

Please cite this article as: H. Chen, X. Yang, Z. Yu, Z. Cheng, H. Yuan, Z. Zhao, G. Wu, N. Xie, X. Yuan, Q. Sun, W. Zhang, Synthesis and biological evaluation of α-santonin derivatives as anti-hepatoma agents, *European Journal of Medicinal Chemistry* (2018), doi: 10.1016/j.ejmech.2018.02.073.

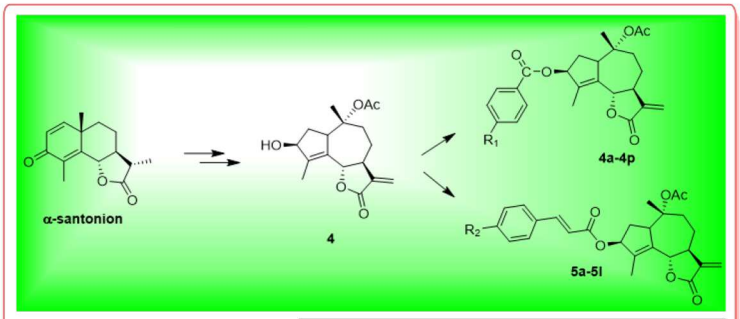

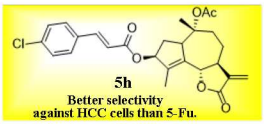

Compd.	IC$_{50}$ (μM)			
	HepG-2	QGY-7703	SMMC-7721	QSG-7701
5h	7.51	3.06	4.08	>100
5-Fu	15.74	14.20	12.47	6.92

Synthesis and biological evaluation of *α*-santonin derivatives as anti-hepatoma agents

Hao Chen[a,c,†], Xiao Yang[a,†], Zongmin Yu[a,†], Ziying Cheng[a], Hu Yuan[b], Zeng Zhao[a,c], Guozhen Wu[a], Ning Xie[c], Xing Yuan[a,*], Qingyan Sun[b,*], Weidong Zhang[a,b,*]

[a]School of Pharmacy, Second Military Medical University, Shanghai 200433, China.

[b]Shanghai Institute of Pharmaceutical Industry, Shanghai 200040, China.

[c]State Key Laboratory of Innovative Natural Medicine and TCM Injections, Jiangxi Qingfeng Pharmaceutical Co., Ltd. Ganzhou 341000, Jiangxi, China.

[†]These authors contributed equally to this work.

*Correspondence:

Weidong Zhang, phone/fax: +86-21-81871244, Email: wdzhangy@hotmail.com.

Qingyan Sun, phone/fax: +86-21-20572000-2030, Email: sqy_2000@163.com.

Xing Yuan, phone/fax: +86-21-81871251, Email: yuanxing2012@126.com.

Abstract

A series of α-santonin-derived compounds as potentially anti-hepatoma agents were designed and synthesized in an effort to find novel therapeutic agents. Among them, derivative **5h** was more potent than the positive control 5-fluorouracil (5-Fu) on HepG-2, QGY-7703 and SMMC-7721 with IC_{50} values of 7.51, 3.06 and 4.08 μM, respectively. The structure-activity relationships (SARs) of these derivatives were discussed. In addition, flow cytometry and western blot assay revealed that the derivatives induced hepatoma cells apoptosis by facilitating apoptosis-related proteins expressions. Our findings suggested that these α-santonin-derived analogues hold promise as chemotherapeutic agents for the treatment of human hepatocellular cancer.

Keywords:

α-Santonin-derived analogues, α-Methylene-γ-lactone, Anti-hepatoma, Structure-activity relationships, Apoptotic

1. Introduction

Hepatocellular cancer (HCC) is the fifth most common malignancy worldwide with more than 700,000 cases diagnosed yearly [1]. However, it is the third leading cause of cancer death due to the high mortality and unsatisfactory treatment options available [2,3]. At the initial diagnosis, surgical resection and transplantation are considered a potentially curative modality for HCC [4]. For patients with localized unresectable disease, systemic treatment is the therapeutic approach. Until recently, the RAF inhibitor sorafenib is the only systemic treatment to demonstrate a statistically significant effect. However, it only improves overall survival by

approximately three months in patients with advanced HCC [5] and several side effects are often observed [6]. Therefore, development of novel therapeutic targets and chemotherapeutic agents is urgently needed.

Sesquiterpene lactones (SQLs) are a family of secondary metabolites derived almost exclusively from Asteraceae/Compositae plants [7]. These natural products are known for their potent bioactivities, such as anti-inflammatory [7-10], antiviral [11], antimicrobial [12-13] and antiprotozoal properties [14], as well as cytotoxicity against tumor cells including HCC [15-18]. Among them, artesunate, dimethylaminoparthenolide, and L12ADT peptide prodrug, a derivative of thapsigargin, have currently been evaluated in cancer clinical or preclinical trials (Chart 1) [18]. SQLs' anti-tumor properties have received considerable attention. However, the exact mechanism of how SQLs play a role in inhibiting the proliferation of tumor cells remains unclear [17]. Their cytotoxic activity has been ascribed as dependent on the α-methylene-γ-lactone group, which is prone to react with suitable nucleophiles [19-21]. Some researchers have found that the cytotoxic activities of these compounds have a strong relationship with their inhibitory effect on many thiol-containing enzymes involved in the synthesis and processing of proteins, RNA and DNA [22,23]. In addition, SQLs exert their cytotoxic effects by triggering apoptosis in many types of cell lines [24-27]. For instance, parthenolide (PTL) with an active fragment α-methylene-γ-lactone skeleton was shown to inhibit proliferation and induce apoptosis in various human cancers *in vitro*, including HCC, colorectal cancer, cholangiocarcinoma and pancreatic cancer [28]. So it is very promising in searching

for novel therapeutic agents for human hepatoma from SQLs.

Our previous studies of SQLs synthesized from *α*-santonin were limited to their anti-inflammatory properties [29,30]. Combined with the preceding analysis, an evaluation of the proliferation inhibition effect of these agents against HCC is essential. The present study investigates their cytotoxic effects on HCC cells and the correlations between the structures of the derivatives of guaiane-type sesquiterpene lactone **4** and anti-HCC cells. A series of benzoic acids and cinnamon acids substituted SQLs derivatives (**4a**-**4p** and **5a**-**5l**) were synthesized, some from our recent report. The effects of the prepared compounds on HCC cell apoptosis were further evaluated. Herein, the synthesis and biological evaluation of these derivatives are reported.

2. Results and discussion

2.1 Chemistry

A convenient method for synthesizing guaiane-type sesquiterpene lactone (3*α*S,6*R*,8*S*,9*β*S)-8-hydroxy-6,9-dimethyl-3-methylene-2-oxo-2,3,3*α*,4,5,6,6*α*,7,8,9*β*-decahydroazuleno[4,5-*β*]furan-6-yl acetate (**4**) is shown in **Scheme 1**. First, we intended to build the *α*-methylene group from *α*-santonin to get (3*α*S,5*α*S,9*β*S)-5*α*,9-dimethyl-3-methylene-3*α*,5,5*α*,9*β*-tetrahydronaphtho[1,2-*β*]furan-2,8(3*H*,4*H*)-dione (**2**). Then, compound (3*α*S,6*R*,9*β*S)-6,9-dimethyl-3-methylene-2,8-dioxo-2,3,3*α*,4,5,6,6*α*,7,8,9*β*-decahydroazuleno[4,5-*β*]furan-6-yl acetate (**3**) was obtained utilizing the photochemical reaction of compound **2**. Regrettably, compound **4** was not produced by reducing compound **3**

under $NaBH_4$, and eventually, *α*-methylene-*γ*-butyrolactone was reduced to *α*-methyl-*γ*-butyrolactone, producing (3*S*,3*αS*,6*R*,8*S*,9*βS*)-8-hydroxy-3,6,9-trimethyl-2-oxo-2,3,3*α*,4,5,6,6*α*,7,8,9*β*-decahydroazuleno[4,5-*β*]furan-6-yl acetate (**6**).

Following the method of our previous literature [27], compound **7** was treated with t-butyldimethylsilyl triflate (TBSOTf) to protect the 2-hydroxyl group and compound **8** was obtained. Then, a two-step procedure of selective dehydrogenation of the *α*-methyl-*γ*-lactone moiety was used that included formation of phenylseleno-substituted **8** followed by treatment with hydrogen peroxide (H_2O_2). Finally, deprotection of the TBS group of compound **9** using tetrabutylammonium fluoride (TBAF), the compound **4** was obtained in excellent yield. The structures of the synthesized target compounds were elucidated by ^{1}H NMR, ^{13}C NMR and HRMS. All spectral data were in accordance with assumed structures.

2.2 Pharmacology and structure-activity relationships

All newly synthesized compounds were tested *in vitro* and the percentage inhibition of treated HepG-2 cells at a single dose of 10 *μ*M compared to untreated control cells was quantified. 5-Fu was used as the positive control. The results showed in **Table 1**. Of the 28 compounds tested, most of them exhibited greater than 50% inhibition of HepG-2 cell growth up to a concentration of 10 *μ*M, except for compounds **4c**, **4g**, **5c**, **5e**, **5f**, **5j** and **5l**.

Compound **4** displayed 32.02% inhibition of HepG-2 cell growth at 10 *μ*M concentration. Compared with compound **4**, the inhibition activities of all of the

derivatives were enhanced. We hypothesized that the polar functional group hydroxyl of compound **4** affected the permeability of membrane, which led to depressed inhibition.

Compounds **4b-4h** have methyl-, ethyl-, n-propyl-, n-butyl-, n-amyl-, isopropyl- and tert-butyl- groups at the R_1 position, respectively. All seven of these compounds exhibited significant effects on inhibition of HepG-2 with the exception of compounds **4c** (42.33%) and **4g** (37.86%). Compared to compound **4a**, with a hydrogen atom at the R_1 position, compounds **4b-4h** had lower activities. Furthermore, the activities were reduced when branching of the linear carbon chains were introduced into the R_1 position [**4d** (62.47%) vs **4g** (37.86%) and **4e** (67.53%) vs **4h** (64.41%)]. These results indicated that a suitable length of the carbon chain could increase the activity and steric hindrance affected the activity at R_1 position.

Comparing analogues **4b** (58.47%), **4k** (72.42%) and **5b** (72.03%) to analogues **4i** (53.03%), **4j** (69.25%) and **5d** (61.14%) with respect to structures, the latter have an additional oxygen atom than the former, but the inhibition of HepG-2 cell growth activities of the latter compounds was lower than that of the former compounds. These results indicated that the activities of derivatives were affected by electron cloud density at the R_1 or R_2 position; as the electron cloud density increased, the activities decreased.

Among analogues **4m-4p**, a halogen was introduced into the R_1 position. Compounds **4m** (78.61%), **4n** (72.69%), **4o** (71.06%) and **4p** (60.11%) contain fluorine, chlorine, bromine and iodine, respectively. These results indicate that when

the electronegativity of the halogen reduced, the activity with inhibition of HepG-2 decreased. Interestingly, this rule applies to cinnamic acid derivatives **5g**-**5i**.

Compounds **5b**-**5f**, methyl-, methylthio-, methoxy-, ethoxy- and propoxy- at the R_2 position. Among these five substituent groups, methylthio- was the strongest electron donor, but compound **5c** (36.24%) with methylthio- had the weakest activity on inhibition of HepG-2 at 10 μM. According to the analysis of the structures and activities of **5b**-**5f**, the activity gradually decreased as electron-donating ability at R_2 position enhanced.

Of the 28 derivatives, 21 tested compounds exhibited greater than 50% inhibition of HepG-2 cell growth at a concentration of 10 μM, the exceptions being compounds **4c**, **4g**, **5c**, **5e**, **5f**, **5j** and **5l**. To further study the cytotoxic profile, the 21 compounds were selected for further cytotoxicity investigation at different concentrations against three different types of HCC cells (HepG-2, QGY-7703 and SMMC-7721). In these tests, 5-Fu was used as the positive control. The IC_{50} values of individual compounds for the 5-dose test against each HCC cell line are presented in **Table 2**. These compounds showed more potent activity than **5-Fu** and had lower cytotoxicity. Among the derivatives tested, cinnamic acid derivatives **5h** displayed the most potent cytotoxicity against HepG-2, QGY-7703 and SMMC-7721 with IC_{50} values of 7.51, 3.06, and 4.08 μM. For comparison, the positive control 5-Fu had IC_{50} values of 15.74, 14.20 and 12.47 μM, respectively.

As shown in **Table 2**, which compares IC_{50} values of compounds **4a**, **4b**, **4d**, **4e** and **4f**, the cytotoxicities against HepG-2 and SMMC-7721 gradually decreased with

the extension of the benzoic acid para alkyl side chain. By contrast, the cytotoxicity against QGY-7703 gradually enhanced. Comparing compounds **4b**, **4k**, and **5b** to **4i**, **4j**, and **5d**, respectively, the former compounds showed more potent activities than the latters against the three HCC cell lines. Beginning with structure analysis, the latter group had one more oxygen atom than the former. It concluded that the introduction of oxygen atoms might have a detrimental effect on inhibition potency.

Cytotoxic selectivity against HCC cells is the most important characteristic of the newly synthesized derivatives. Thus, the inhibitory effects of 21 active compounds on the proliferation of normal hepatic cells (QSG-7701) were further examined. According to the data shown in **Table 2**, compared to 5-Fu, all target compounds presented a weak cytotoxic activity toward QSG-7701. Among them, compounds **4a**, **4b**, **4i**, **4l**, **5a**, **5b**, **5d**, **5g**, **5h** and **5i** exhibited better cytotoxic selectivity against the tumor cells and normal cells than the others. So cinnamon acid substituted analogues showed better cytotoxic selectivity than benzoic acid substituted analogues.

To explore the potential mechanisms of antiproliferative effect induced by derivatives of α-santonin, annexin V-FITC and PI staining were used and flow cytometry (FCM) was performed to quantify cell apoptosis (**Fig. 1**). HCC QGY-7703 cells were cultured with **4n** and **5h** at concentrations of 5, 10 and 15 μM, respectively. Treatment with a low concentration (5 μM) of analogues, **4n** and **5h** did not alter the number of apoptotic cells compared to the control group. In contrast, the apoptosis percentage increased significantly after treatment with higher concentrations (10 and 15 μM) of compounds **4n** and **5h**. To further validate the mechanism of

apoptosis-promoting activities, a western blotting assay was used to evaluate apoptosis-related proteins expression, including PARP, pro-caspase 3, cleaved caspase 3 and pro-caspase 9 expression in QGY-7703. Compared to the DMSO control, the expression levels of cleaved PARP and cleaved caspase 3 were increased, while the pro-caspase 3 and pro-caspase 9 were decreased by **4n** and **5h** in dose-dependent manner, which indicated **4n** and **5h** might up-regulate apoptotic-associated proteins (**Fig. 2**). Together, these observations demonstrated that derivatives of α-santonin induced apoptosis by facilitating apoptosis-related proteins expressions.

3. Conclusion

In conclusion, two series of 28 analogues in total were successfully synthesized from α-santonin, and their activities on the inhibition of HCC cells were evaluated. The main bioactive group in their molecular structures is α-methylene-γ-butyrolactones. Thus, most of the analogues showed varying activities against HCC cells. The SAR analysis proved that: (i) the introduction of halogen atoms is beneficial to the activity against HCC cells, for instance, derivatives **4m**-**4p** (compared to **4a**) and **4m**-**4p** (compared to **5a**); (ii) the introduction of oxygen atoms at R_1 or R_2 position had a detrimental effect on inhibition potency such as derivatives **4i**, **5e**, **5f** and **5l**; (iii) cinnamon acid substituted analogues showed better cytotoxic selectivity than benzoic acid substituted analogues. Among these analogues, **4a**, **4b**, **4i**, **4l**, **5a**, **5b**, **5d**, **5g**, **5h** and **5i** had selective inhibitory activity against HCC cells. Furthermore, derivatives **4n** and **5h** induced significant apoptosis effects in human HCC QGY-7703 cells. These derivatives, especially **5h**, presented better cytotoxic

selectivity for HCC cells, suggesting their potential in targeted chemotherapy for HCC. Further lead optimization and mechanism studies are thus worth pursuing.

4. Experimental section

4.1 Chemistry

Nuclear magnetic resonance (NMR) spectra were recorded using TMS as the internal standard in $CDCl_3$ with a Bruker BioSpin GmbH spectrometer at 500 MHz. The names of these compounds are all generated by Chemdraw Version 14.0 (CambridgeSoft, Cambridge, Mass.). When peak multiplicities are reported, the following abbreviations are used: s = singlet, d = doublet, t = triplet, m = multiplet, and dd = doublet of doublets. Melting points were determined using an X-4B micromelting point apparatus. HRMS was recorded on an Agilent 6520 LC-Q-TOF/MS. Flash column chromatography was performed using silica gel (100–200 and 200–300 mesh). All solvents and reagents were of analytical pure grade, and no further purification needed. All starting materials were commercially available. The spectroscopic data of intermediates **5** and **6** were given in Ref. 29. The spectroscopic data of intermediates **4**, **7**, **8**, **9** and derivatives **4a**, **4b**, **4i**, **4l**, **4n**, **4o**, **5a**, **5b**, **5f**, **5h**, **5i**, **5j** were given in Ref. 30.

*4.1.1 (3R,3αR,5αS,9βS)-3,5α,9-Trimethyl-3-(phenylselanyl)-3α,5,5α,9β-tetrahydro -naphtho[1,2-β]furan-2,8(3H,4H)-dione (**1**)*

To a stirred -78 ºC solution of *α*-santonin (0.246 g, 1.0 mmol, 1.0 equiv) in dry THF (5 mL) under argon, LDA (2.0 M, 0.6 mL, 1.2 equiv) was added dropwise via syringe over 5 min. After 30 min, a solution of PhSeCl (0.211 g, 1.1 mmol, 1.1 equiv) in dry

THF (10 mL) was added dropwise via syringe to the above mixture while keeping internal temperature between -55−-78 ºC. The reaction solution was stirred at -78 °C for 60 min and then at room temperature for overnight. The completion of the reaction was detected by TLC and then quenched by addition of saturated aqueous NH_4Cl. The mixture was extracted with EtOAc three times (3 × 10 mL) and washed with brine. The combined organic layers were dried by anhydrous Na_2SO_4 and evaporated under vacuum to give a residue that was purified by silica-gel column chromatography (PE/EtOAc=25:1−20:1−15:1), resulting in a white solid product **1** (0.30 g, 75%), mp 198.3−199.4 °C. ^{1}H NMR (500 MHz, $CDCl_3$) δ 7.65 (d, J = 7.3 Hz, 2H), 7.44 (d, J = 7.4 Hz, 1H), 7.35 (t, J = 7.5 Hz, 2H), 6.68 (d, J = 9.9 Hz, 1H), 6.25 (d, J = 9.9 Hz, 1H), 5.22 (d, J = 9.6 Hz, 1H), 2.14 (s, 3H), 2.02 – 1.95 (m, 4H), 1.60 (s, 3H), 1.53 (dd, J = 13.4, 7.6 Hz, 1H), 1.33 (s, 3H); ^{13}C NMR (125 MHz, $CDCl_3$) δ 186.2, 174.7, 154.7, 150.9, 138.2 (2×C), 130.0, 129.3 (3×C), 126.0, 123.9, 79.3, 57.6, 48.8, 41.3, 37.5, 25.1, 22.3, 20.6, 11.0. The spectroscopic data are consistent with the values reported in the literature [27].

*4.1.2 (3αS,5αS,9βS)-5α,9-Dimethyl-3-methylene-3α,5,5α,9β-tetrahydronaphtho[1,2-β]furan-2,8(3H,4H)-dione (**2**)*

To a solution of compound **1** (0.4 g, 1.0 mmol, 1.0 equiv) and acetic acid (HAc) (0.13 g, 3.0 mmol, 3.0 equiv）in THF (5 mL) cooled to 0 ºC, 30% H_2O_2 (0.74 mL, 6.5 mmol, 6.5 equiv) was added dropwise. The reaction solution was stirred at 0 ºC for 20 min and then at 20 ºC for 10 min. The reaction was complete detected by TLC and then quenched by addition of saturated aqueous $NaHCO_3$. The mixture was extracted with

EtOAc three times (3 × 10 mL) and washed with brine. The combined organic layers were dried by anhydrous Na_2SO_4 and evaporated under vacuum to give a residue that was purified by silica-gel column chromatography (PE/EtOAc = 15:1 – 10:1 – 8:1), resulting in a white solid product **2** (0.22 g, 90%); mp 200.6−201.4 °C. ^{1}H NMR (500 MHz, $CDCl_3$) δ 6.71 (td, J = 3.1, 9.9 Hz, 1H), 6.28 (d, J = 9.9 Hz, 1H), 6.14 (dd, J = 3.1, 3.3 Hz, 1H), 5.50 (dd, J = 3.1, 3.3 Hz, 1H), 4.78 (d, J = 11.4 Hz, 1H), 2.80 (ttd, J = 3.3, 7.2, 11.4 Hz, 1H), 2.17 (s, 3H), 2.18 (tdd, J = 6.9, 7.2, 14.1 Hz, 1H), 1.88 (dtd, J = 3.1, 6.9, 13.8 Hz, 1H), 1.85 (tdd, J = 6.9, 7.2, 14.1 Hz, 1H), 1.68 (dtd, J = 3.1, 6.9, 13.8 Hz, 1H), 1.32 (s, 3H); ^{13}C NMR (125 MHz, $CDCl_3$) δ 185.9, 168.8, 155.4, 154.4, 138.0, 132.5, 126.1, 119.5, 81.3, 45.7, 40.2, 36.8, 25.0, 23.6, 11.3. The spectroscopic data are consistent with the values reported in the literature [27].

*4.1.3 (3αS,6R,9βS)-6,9-Dimethyl-3-methylene-2,8-dioxo-2,3,3α,4,5,6,6α,7,8,9β-deca -hydroazuleno[4,5-β]furan-6-yl acetate (**3**)*

A solution of compound **2** (10 g, 41.0 mmol) in glacial AcOH (400 mL) was irradiated under argon at 17 °C for 12 h using a 500 W high-pressure mercury arc lamp. After the AcOH was evaporated in vacuum, diethyl ether (20 mL) was added to the resulting residue. Filtration of the precipitate afforded **3** (4.48 g, 36%) as a colorless solid, mp 100.7−101.2 °C. ^{1}H NMR (500 MHz, $CDCl_3$) δ 6.34 (d, J = 3.2, 1H), 5.61 (d, J = 3.2, 1H), 4.80 (d, J = 10.9, 1H), 4.21 (dd, J = 6.2, J = 2.6, 1H), 3.14 (m, 1H), 2.68 (m, 1H), 2.54 (dd, J = 19.3, J = 6.2, 1H), 2.43 (dd, J = 19.3, J = 2.6, 1H), 2.20–2.34 (m, 2H), 2.01 (s, 3H), 1.95 (s, 3H), 1.46–1.56 (m, 1H), 1.13 (s, 3H); ^{13}C NMR (125 MHz, $CDCl_3$): δ 206.8, 170.4, 168.8, 160.3, 143.2, 137.6, 120.8, 85.5,

81.7, 47.3, 44.5, 37.5, 36.9, 24.5, 22.3, 20.0, 9.6; The spectroscopic data are consistent with the values reported in the literature [27].

*4.1.4 General procedure for syntheses of derivatives **4a-4p** and **5a-5l***

To a solution of compound **4** (20 mg, 0.065 mmol) and acid (0.065 mmol) in DCM (10 mL) at room temperature was added DMAP (15.9 mg, 0.13 mmol). After stirring for 10 min, EDCI (25.0 mg, 0.13 mmol) was added in one portion. The reaction was allowed to stir overnight. Then, water (10 mL) was added. The reaction mixture was extracted with DCM (3×10 mL). The organic layer was then washed with brine, dried over Na_2SO_4, and concentrated in vacuum. Purification by flash column chromatography (PE: EtOAc = 4:1) provided the derivatives of interest.

*4.1.4.1 (3αS,6R,8S,9βS)-6-Acetoxy-6,9-dimethyl-3-methylene-2-oxo-2,3,3α,4,5,6,6α,-7,8,9β-decahydroazuleno[4,5-β]furan-8-yl 4-ethylbenzoate (**4c**)*

Colorless solid; mp 145.1−146.3 °C; yield 79%: ^{1}H NMR (500 MHz, $CDCl_3$) δ 7.97 (d, J = 8.3 Hz, 2H), 7.28 (s, 1H), 7.27 (s, 1H), 6.26 (d, J = 3.3 Hz, 1H), 5.75 (d, J = 6.6 Hz, 1H), 5.53 (d, J = 3.1 Hz, 1H), 4.70 (dd, J = 11.0, 1.7 Hz, 1H), 4.30 (t, J = 6.7 Hz, 1H), 3.92 (s, 1H), 2.75 – 2.68 (m, 3H), 1.97 (s, 1H), 1.96 (s, 3H), 1.95 (s, 3H), 1.27 (s, 1H), 1.26 (s, 3H), 1.25 (s, 2H), 1.24 (s, 4H); ^{13}C NMR (125 MHz, $CDCl_3$) δ 170.3, 169.6, 166.3, 141.2, 138.4, 133.2, 130.9, 129.7 (2×C), 128.8, 128.0 (2×C), 119.8, 86.2, 81.6, 80.4, 52.2, 45.1, 37.4, 32.2, 29.0, 24.2, 22.4, 20.0, 15.3, 12.9; HRMS (ESI): m/z calcd for $C_{26}H_{31}O_6$ $[M+H]^+$: 439.2115, found 439.2116.

*4.1.4.2 (3αS,6R,8S,9βS)-6-acetoxy-6,9-dimethyl-3-methylene-2-oxo-2,3,3α,4,5,6,6α,7,8,9β-decahydroazuleno[4,5-β]furan-8-yl 4-propylbenzoate (**4d**)*

Colorless solid; mp 150.5−151.7 °C; yield 82%: ^{1}H NMR (500 MHz, $CDCl_3$) δ 7.96 (d, *J* = 8.3 Hz, 2H), 7.26 – 7.26 (m, 1H), 7.24 (s, 1H), 6.26 (d, *J* = 3.3 Hz, 1H), 5.76 (t, *J* = 6.1 Hz, 1H), 5.53 (d, *J* = 3.1 Hz, 1H), 4.70 (dd, *J* = 10.9, 1.8 Hz, 1H), 3.92 (s, 1H), 3.00 – 2.91 (m, 1H), 2.69 – 2.60 (m, 3H), 2.50 (td, *J* = 13.4, 4.2 Hz, 1H), 2.24 (ddd, *J* = 18.3, 13.7, 3.6 Hz, 2H), 1.95 (d, *J* = 4.6 Hz, 6H), 1.66 (dd, *J* = 15.0, 7.5 Hz, 3H), 1.24 (s, 4H), 0.94 (t, *J* = 7.4 Hz, 3H); ^{13}C NMR (125 MHz, $CDCl_3$) δ 170.3, 166.3, 148.5, 141.2, 138.4, 133.2, 129.6 (2×C), 128.6 (2×C), 127.7, 119.8, 86.2, 81.6, 80.4, 52.2, 45.1, 38.0, 37.4, 32.2, 24.2, 24.2, 22.4, 20.0, 13.7, 12.9; HRMS (ESI): m/z calcd for $C_{27}H_{33}O_6$ $[M+H]^+$: 453.2272, found 453.2276.

*4.1.4.3 (3αS,6R,8S,9βS)-6-acetoxy-6,9-dimethyl-3-methylene-2-oxo-2,3,3α,4,5,6,6α, 7,8,9β-decahydroazuleno[4,5-β]furan-8-yl 4-butylbenzoate (**4e**)*

Colorless solid; mp 165.2−166.8 °C; yield 85%: ^{1}H NMR (500 MHz, $CDCl_3$) δ 7.96 (t, *J* = 5.8 Hz, 2H), 7.25 (s, 2H), 6.27 (t, *J* = 2.8 Hz, 1H), 5.76 (t, *J* = 6.1 Hz, 1H), 5.53 (d, *J* = 3.1 Hz, 1H), 4.70 (dd, *J* = 10.9, 1.7 Hz, 1H), 3.92 (s, 1H), 2.99 – 2.92 (m, 1H), 2.69 – 2.61 (m, 3H), 2.50 (td, *J* = 13.4, 4.2 Hz, 1H), 2.30 – 2.18 (m, 2H), 1.95 (d, *J* = 4.8 Hz, 6H), 1.78 – 1.73 (m, 1H), 1.63 – 1.59 (m, 2H), 1.35 (dd, *J* = 15.0, 7.5 Hz, 2H), 1.25 (d, *J* = 6.5 Hz, 4H), 0.93 (t, *J* = 7.4 Hz, 3H); ^{13}C NMR (125 MHz, $CDCl_3$) δ 170.3, 169.6, 166.3, 148.7, 141.2, 138.4, 133.2, 129.6 (2×C), 128.5 (2×C), 127.7, 119.8, 86.2, 81.6, 80.4, 52.2, 45.1, 37.4, 35.7, 33.3, 32.2, 24.2, 22.3, 22.3, 20.0, 13.9, 12.9; HRMS (ESI): m/z calcd for $C_{28}H_{35}O_6$ $[M+H]^+$: 467.2428, found 467.2435.

*4.1.4.4 (3αS,6R,8S,9βS)-6-acetoxy-6,9-dimethyl-3-methylene-2-oxo-2,3,3α,4,5,6,6α, 7,8,9β-decahydroazuleno[4,5-β]furan-8-yl 4-pentylbenzoate (**4f**)*

Colorless solid; mp 170.2−172.1 °C; yield 77%: ^{1}H NMR (500 MHz, $CDCl_3$) δ 7.96 (d, *J* = 8.3 Hz, 2H), 7.24 (s, 2H), 6.26 (d, *J* = 3.3 Hz, 1H), 5.76 (t, *J* = 5.7 Hz, 1H), 5.53 (d, *J* = 3.1 Hz, 1H), 4.70 (dd, *J* = 10.9, 1.7 Hz, 1H), 3.92 (s, 1H), 2.95 (dd, *J* = 10.8, 9.6 Hz, 1H), 2.66 (t, *J* = 7.8 Hz, 3H), 2.50 (td, *J* = 13.3, 4.2 Hz, 1H), 2.30 – 2.25 (m, 1H), 2.24 – 2.18 (m, 1H), 1.95 (d, *J* = 4.6 Hz, 6H), 1.79 – 1.72 (m, 1H), 1.65 – 1.61 (m, 2H), 1.50 – 1.40 (m, 1H), 1.34 (d, *J* = 1.4 Hz, 1H), 1.25 (d, *J* = 6.5 Hz, 6H), 0.89 (t, *J* = 9.6, 4.3 Hz, 3H); ^{13}C NMR (125 MHz, $CDCl_3$) δ 170.3, 169.6, 166.3, 148.8, 141.2, 138.4, 133.2, 129.6 (2×C), 128.5 (2×C), 127.7, 119.8, 86.2, 81.6, 80.4, 52.2, 45.1, 37.4, 36.0, 32.2, 31.4, 30.8, 29.7, 24.2, 22.5, 20.0, 14.0, 12.9; HRMS (ESI): m/z calcd for $C_{29}H_{37}O_6$ $[M+H]^+$: 481.2585, found 481.2585.

*4.1.4.5 (3αS,6R,8S,9βS)-6-acetoxy-6,9-dimethyl-3-methylene-2-oxo-2,3,3α,4,5,6,6α, 7,8,9β-decahydroazuleno[4,5-β]furan-8-yl 4-isopropylbenzoate (**4g**)*

Colorless solid; mp 140.9−142.3 °C; yield 69%: ^{1}H NMR (500MHz, $CDCl_3$) δ 8.03 (d, *J* = 8.0 Hz, 1H), 8.03 (d, *J* = 8.0 Hz, 1H), 7.21 (d, *J* = 8.0 Hz, 1H), 7.21 (d, *J* = 8.0 Hz, 1H), 6.27 (dd, *J* = 3.1, 3.2 Hz, 1H), 5.85 (t, *J* = 14.0 Hz, 1H), 5.51 (dd, *J* = 3.0, 3.1 Hz, 1H), 4.60 (d, *J* = 10.7 Hz, 1H), 3.49 (dd, *J* = 7.4, 10.6 Hz, 1H), 2.97 (spt, *J* = 6.9 Hz, 1H), 2.95 (dddt, *J* = 3.0, 3.2, 10.7, 10.8 Hz, 1H), 2.40 (ddd, *J* = 7.4, 13.2, 14.0 Hz, 1H), 2.24 (ddd, *J* = 8.3, 9.3, 13.9 Hz, 1H), 2.14 (dddd, *J* = 8.3, 9.3, 10.8, 12.6 Hz, 1H), 1.97 (s, 3H), 1.83 (s, 3H), 1.86 (ddd, *J* = 9.3, 12.4, 13.9 Hz, 1H), 1.82 (ddd, *J* = 10.6, 13.2, 14.0 Hz, 1H), 1.64 (dddd, *J* = 9.3, 10.8, 12.4, 12.6 Hz, 1H), 1.24 (d, *J* = 6.9 Hz, 6H), 1.22 (s, 3H); ^{13}C NMR (125 MHz, $CDCl_3$) δ 171.7, 168.1, 166.4, 152.0, 142.4, 139.7, 132.3, 129.4, 129.4, 126.9, 125.8, 125.8, 118.8, 86.8, 81.4, 81.3, 51.9, 45.5,

37.3, 34.1, 32.4, 24.5, 23.3, 23.3, 22.5, 20.0, 12.2; HRMS (ESI): m/z calcd for $C_{27}H_{32}O_6Na$ $[M+Na]^+$: 475.2091, found 475.2108.

*4.1.4.6 (3αS,6R,8S,9βS)-6-acetoxy-6,9-dimethyl-3-methylene-2-oxo-2,3,3α,4,5,6,6α,7,8,9β-decahydroazuleno[4,5-β]furan-8-yl 4-(tert-butyl)benzoate (**4h**)*

Colorless solid; mp 148.7−149.5 °C; yield 86%: ^{1}H NMR (500 MHz, $CDCl_3$) δ 7.99 (d, *J* = 8.5 Hz, 2H), 7.47 (d, *J* = 8.5 Hz, 2H), 6.27 (t, *J* = 3.1 Hz, 1H), 5.80 – 5.72 (m, 1H), 5.53 (d, *J* = 3.0 Hz, 1H), 4.70 (dd, *J* = 10.9, 1.7 Hz, 1H), 3.93 (s, 1H), 2.96 (dd, *J* = 10.8, 9.7 Hz, 1H), 2.65 (dt, *J* = 14.7, 8.3 Hz, 1H), 2.50 (dt, *J* = 13.2, 6.6 Hz, 1H), 2.29 – 2.19 (m, 2H), 1.95 (d, *J* = 4.7 Hz, 6H), 1.78 – 1.72 (m, 1H), 1.49 (s, 1H), 1.34 (s, 9H), 1.24 (s, 3H); ^{13}C NMR (125 MHz, $CDCl_3$) δ 170.3, 169.6, 166.2, 156.8, 141.2, 138.4, 133.2, 129.47 (2×C), 127.5, 125.40 (2×C), 119.7, 86.2, 81.5, 80.4, 52.2, 45.1, 37.4, 35.1, 32.2, 31.1 (3×C), 24.2, 22.4, 20.0, 12.9; HRMS (ESI): m/z calcd for $C_{28}H_{34}O_6Na$ $[M+Na]^+$: 489.2248, found 489.2252.

*4.1.4.7 (3αS,6R,8S,9βS)-6-acetoxy-6,9-dimethyl-3-methylene-2-oxo-2,3,3α,4,5,6,6α,7,8,9β-decahydroazuleno[4,5-β]furan-8-yl 4-(trifluoromethoxy)benzoate (**4j**)*

Colorless solid; mp 138.2−139.9 °C; yield 76%: ^{1}H NMR (500 MHz, $CDCl_3$) δ 8.10 (d, *J* = 8.8 Hz, 2H), 7.28 (d, *J* = 8.3 Hz, 2H), 6.27 (d, *J* = 3.3 Hz, 1H), 5.77 (t, *J* = 5.7 Hz, 1H), 5.54 (d, *J* = 3.0 Hz, 1H), 4.69 (dd, *J* = 10.9, 1.6 Hz, 1H), 3.94 (s, 1H), 2.95 (t, *J* = 10.3 Hz, 1H), 2.65 (dt, *J* = 14.7, 8.2 Hz, 1H), 2.51 (td, *J* = 13.3, 4.2 Hz, 1H), 2.30 – 2.21 (m, 2H), 1.96 (s, 3H), 1.94 (s, 3H), 1.79 – 1.72 (m, 1H), 1.51 – 1.41 (m, 1H), 1.23 (s, 3H); ^{13}C NMR (125 MHz, $CDCl_3$) δ 170.3, 169.5, 165.0, 152.7, 140.7, 138.3, 133.6, 131.6 (2×C), 128.6, 121.3, 120.3 (2×C), 119.9, 86.1, 81.5, 81.0, 52.2, 45.1,

37.4, 32.2, 24.2, 22.4, 20.0, 12.9; HRMS (ESI): m/z calcd for $C_{25}H_{26}F_3O_7$ $[M+H]^+$: 495.1625, found 495.1617.

*4.1.4.8 (3αS,6R,8S,9βS)-6-acetoxy-6,9-dimethyl-3-methylene-2-oxo-2,3,3α,4,5,6,6α,7,8,9β-decahydroazuleno[4,5-β]furan-8-yl 4-(trifluoromethyl)benzoate (**4k**)*

Colorless solid; mp 129.7−131.5 °C; yield 84%: ^{1}H NMR (500 MHz, $CDCl_3$) δ 8.17 (d, J = 8.1 Hz, 2H), 7.72 (d, J = 8.3 Hz, 2H), 6.27 (d, J = 3.2 Hz, 1H), 5.80 (s, 1H), 5.54 (d, J = 2.8 Hz, 1H), 4.70 (d, J = 11.0 Hz, 1H), 3.95 (s, 1H), 2.96 (t, J = 10.5 Hz, 1H), 2.67 (dt, J = 16.1, 8.2 Hz, 1H), 2.58 – 2.47 (m, 1H), 2.31 – 2.18 (m, 2H), 1.96 (s, 3H), 1.95 (s, 3H), 1.77 (d, J = 14.6 Hz, 1H), 1.52 – 1.39 (m, 1H), 1.24 (s, 3H); ^{13}C NMR (125 MHz, $CDCl_3$) δ 170.3, 169.5, 165.0, 140.5, 138.3, 133.8, 133.4, 130.0 (3×C), 125.5 (3×C), 119.9, 86.1, 81.5, 81.3, 52.1, 45.1, 37.4, 32.1, 24.2, 22.4, 20.0, 12.9; HRMS (ESI): m/z calcd for $C_{25}H_{25}F_3O_6Na$ $[M+Na]^+$: 501.1495, found 501.1514.

*4.1.4.9 (3αS,6R,8S,9βS)-6-acetoxy-6,9-dimethyl-3-methylene-2-oxo-2,3,3α,4,5,6,6α,7,8,9β-decahydroazuleno[4,5-β]furan-8-yl 4-fluorobenzoate (**4m**)*

Colorless solid; mp 173.2−174.8 °C; yield 74%: ^{1}H NMR (500 MHz, $CDCl_3$) δ 8.07 (dd, J = 8.2, 5.6 Hz, 2H), 7.12 (t, J = 8.5 Hz, 2H), 6.27 (d, J = 3.0 Hz, 1H), 5.76 (s, 1H), 5.54 (d, J = 2.6 Hz, 1H), 4.70 (d, J = 10.6 Hz, 1H), 3.93 (s, 1H), 2.95 (t, J = 10.4 Hz, 1H), 2.72 – 2.45 (m, 2H), 2.33 – 2.17 (m, 2H), 1.96 (d, J = 8.9 Hz, 6H), 1.79 – 1.70 (m, 1H), 1.49 – 1.42 (m, 1H), 1.24 (s, 3H); ^{13}C NMR (125 MHz, $CDCl_3$) δ 170.3, 169.5, 165.3, 140.9, 138.4, 133.4 (2×C), 132.1 (2×C), 119.8, 115.7, 115.5, 86.1, 81.5, 80.8, 52.1, 45.0, 37.4, 32.2, 29.7, 24.2, 22.4, 20.0, 12.9; HRMS (ESI): m/z calcd for

$C_{24}H_{26}FO_6$ $[M+H]^+$: 429.1708, found 429.1706.

*4.1.4.10 (3α*S*,6R,8S,9β*S*)-6-acetoxy-6,9-dimethyl-3-methylene-2-oxo-2,3,3α,4,5,6,6α,7,8,9β-decahydroazuleno[4,5-β]furan-8-yl 4-iodobenzoate (**4p**)*

Colorless solid; mp 190.2−191.1 °C; yield 89%: ^{1}H NMR (500 MHz, $CDCl_3$) δ 7.81 (d, *J* = 8.6 Hz, 2H), 7.75 (d, *J*= 8.6 Hz, 2H), 6.26 (d, *J* = 3.3 Hz, 1H), 5.75 (t, *J* = 6.2 Hz, 1H), 5.53 (d, *J* = 3.1 Hz, 1H), 4.69 (dd, *J* = 10.9, 1.7 Hz, 1H), 3.93 (s, 1H), 2.98 – 2.91 (m, 1H), 2.64 (dt, *J* = 14.6, 8.2 Hz, 1H), 2.51 (td, *J* = 13.3, 4.2 Hz, 1H), 2.26 (dt, *J* = 18.5, 4.4 Hz, 2H), 1.96 (s, 3H), 1.93 (s, 3H), 1.77 – 1.71 (m, 1H), 1.50 – 1.41 (m, 1H), 1.23 (s, 3H); ^{13}C NMR (125 MHz, $CDCl_3$) δ 170.3, 169.5, 165.8, 140.8, 138.3, 137.8 (2×C), 133.6, 131.0 (2×C), 129.7, 119.9, 100.9, 86.1, 81.5, 80.9, 52.1, 45.1, 37.4, 32.2, 24.2, 22.4, 20.0, 12.9; HRMS (ESI): m/z calcd for $C_{24}H_{26}IO_6$ $[M+H]^+$: 537.0769, found 537.0767.

*4.1.4.11 (3α*S*,6R,8S,9β*S*)-6-acetoxy-6,9-dimethyl-3-methylene-2-oxo-2,3,3α,4,5,6,6α,7,8,9β-decahydroazuleno[4,5-β]furan-8-yl (E)-3-(4-(methylthio)phenyl)acrylate (**5c**)*

Colorless solid; mp 150.3−151.7 °C; yield 84%: ^{1}H NMR (500 MHz, $CDCl_3$) δ 7.66 (d, *J* = 15.8 Hz, 1H), 7.48 – 7.41 (m, 2H), 7.23 (d, *J* = 8.4 Hz, 2H), 6.40 (t, *J* = 16.4 Hz, 1H), 6.26 (t, *J* = 3.1 Hz, 1H), 5.74 – 5.64 (m, 1H), 5.53 (d, *J* = 3.0 Hz, 1H), 4.72 – 4.56 (m, 1H), 3.89 (s, 1H), 2.94 (t, *J* = 10.2 Hz, 1H), 2.60 (dt, *J* = 14.6, 8.3 Hz, 1H), 2.51 (d, *J* = 1.6 Hz, 4H), 2.27 – 2.17 (m, 2H), 1.98 (s, 1H), 1.97 (s, 3H), 1.95 (s, 1H), 1.92 (s, 2H), 1.85 (d, *J* = 16.6 Hz, 1H), 1.23 (s, 3H); ^{13}C NMR (125 MHz, $CDCl_3$) δ 170.3, 169.6, 166.8, 144.6, 142.1, 141.2, 138.5, 133.0, 130.8, 128.5 (2×C), 126.0

(2×C), 119.8, 116.9, 86.2, 81.6, 80.0, 52.1, 45.1, 37.5, 32.2, 24.2, 22.4, 20.0, 15.1, 12.9; HRMS (ESI): m/z calcd for $C_{27}H_{30}O_6SNa$ $[M+Na]^+$: 505.1655, found 505.1648.

*4.1.4.12 (3α*S*,6R,8S,9β*S*)-6-acetoxy-6,9-dimethyl-3-methylene-2-oxo-2,3,3α,4,5,6,6α, 7,8,9β-decahydroazuleno[4,5-β]furan-8-yl (E)-3-(4-methoxyphenyl)acrylate (**5d**)*

Colorless solid; mp 135.4−137.2 °C; yield 81%: ^{1}H NMR (500 MHz, $CDCl_3$) δ 7.67 (d, J = 15.8 Hz, 1H), 7.49 (d, J = 8.7 Hz, 2H), 6.94 – 6.88 (m, 2H), 6.33 (d, J = 16.0 Hz, 1H), 6.26 (d, J = 3.3 Hz, 1H), 5.66 (t, J = 6.7 Hz, 1H), 5.54 – 5.50 (m, 1H), 4.65 (ddd, J = 33.0, 11.0, 1.7 Hz, 1H), 3.89 (dd, J = 5.4, 3.6 Hz, 1H), 3.84 (d, J = 2.0 Hz, 3H), 2.94 (dd, J = 10.9, 9.5 Hz, 1H), 2.64 – 2.44 (m, 2H), 2.28 – 2.18 (m, 2H), 1.98 (s, 1H), 1.97 (s, 2H), 1.95 (s, 1H), 1.92 (s, 2H), 1.72 – 1.69 (m, 1H), 1.44 (dd, J = 10.0, 7.2 Hz, 1H), 1.23 (s, 2H), 1.14 (s, 1H); ^{13}C NMR (125 MHz, $CDCl_3$) δ 170.3, 169.6, 167.0, 161.5, 144.8, 138.5, 132.9, 129.8 (2×C), 127.1, 119.8, 115.4, 114.4 (2×C), 86.2, 81.6, 79.9, 55.4, 52.1, 45.1, 37.5, 32.3, 29.7, 24.2, 22.4, 20.0, 12.9; HRMS (ESI): m/z calcd for $C_{27}H_{30}O_7Na$ $[M+Na]^+$: 489.1883, found 489.1881.

*4.1.4.13 (3α*S*,6R,8S,9β*S*)-6-acetoxy-6,9-dimethyl-3-methylene-2-oxo-2,3,3α,4,5,6,6α, 7,8,9β-decahydroazuleno[4,5-β]furan-8-yl (E)-3-(4-ethoxyphenyl)acrylate (**5e**)*

Colorless solid; mp 141.2−143.1 °C; yield 80%: ^{1}H NMR (500 MHz, $CDCl_3$) δ 7.66 (d, J = 15.8 Hz, 1H), 7.47 (d, J = 8.7 Hz, 2H), 6.91 – 6.86 (m, 2H), 6.32 (d, J = 16.0 Hz, 1H), 6.26 (d, J = 3.2 Hz, 1H), 5.73 – 5.63 (m, 1H), 5.52 (d, J = 3.1 Hz, 1H), 4.68 (d, J = 12.5 Hz, 1H), 4.07 (q, J = 7.0 Hz, 2H), 3.87 (d, J = 16.5 Hz, 1H), 2.94 (t, J = 10.6 Hz, 1H), 2.62 – 2.55 (m, 1H), 2.30 – 2.27 (m, 1H), 2.20 (d, J = 4.6 Hz, 1H), 1.97 (s, 3H), 1.94 (s, 1H), 1.92 (s, 2H), 1.87 (s, 1H), 1.73 – 1.67 (m, 1H), 1.64 – 1.58 (m,

1H), 1.44 – 1.41 (m, 3H), 1.23 (s, 3H); ^{13}C NMR (125 MHz, $CDCl_3$) δ 170.3, 169.6, 167.1, 160.9, 144.9, 141.3, 138.5, 132.9, 129.8 (2×C), 126.9, 119.8, 115.3, 114.8 (2×C), 86.2, 81.6, 79.8, 63.6, 52.1, 45.1, 37.5, 32.3, 29.7, 24.2, 22.4, 20.0, 14.7, 12.8; HRMS (ESI): m/z calcd for $C_{28}H_{33}O_7$ $[M+H]^+$: 481.2221, found 481.2220.

*4.1.4.14 (3αS,6R,8S,9βS)-6-acetoxy-6,9-dimethyl-3-methylene-2-oxo-2,3,3α,4,5,6,6α, 7,8,9β-decahydroazuleno[4,5-β]furan-8-yl (E)-3-(4-fluorophenyl)acrylate (**5g**)*

Colorless solid; mp 129.7−131.5 °C; yield 91%: ^{1}H NMR (500 MHz, $CDCl_3$) δ 7.67 (d, *J* = 16.0 Hz, 1H), 7.52 (dd, *J* = 8.7, 5.4 Hz, 2H), 7.08 (t, *J* = 8.6 Hz, 2H), 6.39 (d, *J* = 16.0 Hz, 1H), 6.26 (d, *J* = 3.3 Hz, 1H), 5.69 (dt, *J* = 12.6, 6.1 Hz, 1H), 5.53 (d, *J* = 3.0 Hz, 1H), 4.68 (dd, *J* = 10.9, 1.8 Hz, 1H), 3.90 (s, 1H), 2.94 (dd, *J* = 10.8, 9.5 Hz, 1H), 2.50 (td, *J* = 13.3, 4.2 Hz, 1H), 2.29 – 2.17 (m, 2H), 1.97 (s, 3H), 1.94 (s, 1H), 1.92 (s, 3H), 1.73 – 1.66 (m, 1H), 1.44 (dd, *J* = 10.9, 3.2 Hz, 1H), 1.23 (s, 3H); ^{13}C NMR (125 MHz, $CDCl_3$) δ 170.3 (2×C), 169.6, 166.6, 165.0, 143.8, 141.0, 133.1, 130.0, 130.0 (2×C), 119.8 (2×C), 117.8, 116.2, 116.0, 86.2, 81.6, 80.1, 52.1, 45.1, 37.5, 32.2, 24.2, 22.4, 20.0, 12.8; HRMS (ESI): m/z calcd for $C_{26}H_{28}FO_6$ $[M+H]^+$: 455.1864, found 455.1861.

*4.1.4.15 (3αS,6R,8S,9βS)-6-acetoxy-6,9-dimethyl-3-methylene-2-oxo-2,3,3α,4,5,6,6α, 7,8,9β-decahydroazuleno[4,5-β]furan-8-yl (E)-3-(4-(trifluoromethyl)phenyl)acrylate (**5k**)*

Colorless solid; mp 140.3−142.1 °C; yield 87%: ^{1}H NMR (500 MHz, $CDCl_3$) δ 7.75 – 7.69 (m, 1H), 7.67 – 7.62 (m, 4H), 6.53 (t, *J* = 9.4 Hz, 1H), 6.28 – 6.24 (m, 1H), 5.75 – 5.64 (m, 1H), 5.52 (dd, *J* = 7.7, 3.0 Hz, 2H), 4.71 – 4.61 (m, 1H), 3.88 (d, *J* = 26.5

Hz, 1H), 2.93 (dd, *J* = 22.6, 11.2 Hz, 1H), 2.61 (dt, *J* = 14.6, 8.2 Hz, 1H), 1.98 (s, 3H), 1.92 (s, 3H), 1.25 (d, *J* = 4.8 Hz, 4H), 1.23 (s, 3H); ^{13}C NMR (125 MHz, $CDCl_3$) δ 170.3, 169.5, 166.1, 143.2, 140.8, 138.4, 137.7, 133.3, 133.0, 128.2 (2×C), 125.9 (2×C), 120.6, 119.9, 86.2, 81.6, 80.4, 52.1, 45.1, 37.5, 32.2, 29.7, 24.2, 22.4, 20.0, 12.8; HRMS (ESI): m/z calcd for $C_{27}H_{27}F_3O_6Na$ $[M+Na]^+$: 527.1652, found 527.1659.

*4.1.4.16 (3αS,6R,8S,9βS)-6-acetoxy-6,9-dimethyl-3-methylene-2-oxo-2,3,3α,4,5,6,6α,7,8,9β-decahydroazuleno[4,5-β]furan-8-yl (E)-3-(4-nitrophenyl)acrylate (**5l**)*

Colorless solid; mp 151.4−152.3 °C; yield 88%: ^{1}H NMR (500 MHz, $CDCl_3$) δ 8.26 (d, *J* = 8.7 Hz, 2H), 7.78 – 7.66 (m, 3H), 6.57 (dd, *J* = 20.4, 16.0 Hz, 1H), 6.27 (t, *J* = 3.2 Hz, 1H), 5.69 (t, *J* = 5.9 Hz, 1H), 5.54 (d, *J* = 3.0 Hz, 1H), 4.72 – 4.59 (m, 1H), 3.92 (s, 1H), 2.62 (dt, *J* = 14.6, 8.2 Hz, 1H), 2.51 (td, *J* = 13.4, 4.2 Hz, 1H), 2.27 – 2.18 (m, 2H), 1.99 – 1.97 (m, 3H), 1.96 (s, 1H), 1.93 (s, 3H), 1.74 – 1.68 (m, 1H), 1.44 (ddd, *J* = 11.0, 8.5, 3.0 Hz, 1H), 1.23 (s, 3H); ^{13}C NMR (125 MHz, $CDCl_3$) δ 170.3 169.5, 165.7, 148.6 142.2 140.7 140.4, 138.3, 133.5, 128.7 (2×C), 124.2 (2×C), 122.3, 119.9, 86.1, 81.5, 80.7 52.1, 45.1 37.4, 32.1, 24.2, 22.4, 20.0, 12.8; HRMS (ESI): m/z calcd for $C_{26}H_{27}NO_8Na$ $[M+Na]^+$: 504.1629, found 504.1620.

4.2 Biological assays

4.2.1 Cell culture

Cells were cultured in media containing 10% FBS, 100 units/ml penicillin, 100 μg/ml streptomycin at 37 °C in a humidified incubator containing 5% CO_2. HCC cell lines QGY-7703, HepG-2 and SMMC-7721 and liver non-tumor cell lines QSG-7701 were

obtained from Cell Bank of the Chinese Academy of Sciences (Shanghai, China). QGY-7703, SMMC-7721 and QSG-7701 cells were maintained in RPMI 1640 medium and HepG-2 cells were maintained in DMEM medium.

4.2.2 Cell proliferation/viability assay

Cell proliferation was measured using a Cell Counting Kit-8 (CCK-8) (Dojindo, Kumamoto, Japan) according to the manufacturer's instructions. In brief, the cells (2×10^5 cells/well in 100 μl fresh medium) were cultivated in 96-well microplates for 24 h, treated with different concentrations of compounds or 1% DMSO as vehicle control. After incubation with dose-related concentrations compounds or 1% DMSO as vehicle control for 24 h, 10 μl of CCK-8 solution was added to each well for additional 1 h incubation before the absorbance was measured at 450 nm by an epoch microplate spectrophotometer.

4.2.3 Flow cytometry analysis

QGY-7703 cells were seeded in 12-well plates (5×10^5 cells/well) for 24 h and then treated with compounds at dose-related concentrations or DMSO for 24 h. The treated cells were stained using Annexin V-FITC/PI apoptosis detection kit (BD Biosciences, San Jose, CA, USA) according to the manufacturer's instructions. After incubation at room temperature for 15 min in the dark, the apoptotic cells were immediately analyzed by flow cytometry (Becton Dickinson FACS Vantage SE, San Jose, CA, USA).

4.2.4 Western blotting analysis

QGY-7703 cells were subcultured in a 6-well plate. After incubation for 24 h, cells

were treated with compounds for 24 h. The cells were lysed in GLO lysis buffer (Promega, USA) supplemented with 1x protease inhibitors (Roche Applied Sciences, Germany). The concentration of protein in the supernatant fractions was measured using the Pierce™ BCA Protein Assay Kit, according to the manufacturer's instructions. Equal amounts of protein were applied to 10 % SDS-polyacrylamide gel and then transferred to PVDF membranes (Bio-Rad). After transfer, the membrane was blocked in 5% fat-free milk for 1 h at RT and incubated with primary antibody for PARP (1:1000; Cell Signaling Technology, Beverly, MA, USA), cleaved caspase 3, pro-caspase 3, pro-caspase 9 (1:1000; Cell Signaling Technology) and GAPDH (1:3000, Beyotime, Shanghai, China) at 4 °C overnight，followed by incubation with a donkey anti-rabbit or a donkey anti-mouse second antibodies (IRDye 800, LI-COR, Biosciences) for 1 h at RT. The image was captured by the Odyssey Infrared Imaging System (LI-COR, Biosciences), according to the manufacturer's instructions. Protein densitometry was performed using Quantity One imaging software (Bio-Rad).

Acknowledgments

The work was supported by Professor of Chang Jiang Scholars Program, NSFC (81230090, 81520108030, 21472238, 81602980), Shanghai Engineering Research Center for the Preparation of Bioactive Natural Products (16DZ2280200), the Scientific Foundation of Shanghai China (12401900801, 13401900103, 13401900101), National Major Project of China (2011ZX09307-002-03)

References

[1] J. Bruix, Hepatocellular carcinoma: clinical frontiers and perspectives, Gut, 63

(2014) 844-855.

[2] P.J. Wysocki, Targeted therapy of hepatocellular cancer, Expert Opin. Invest. Drugs, 19 (2010) 265-274.

[3] Z. Xiao, S.C. Chow, C.H. Li, S.C. Tang, S.K.W. Tsui, Z. Lin, Y. Chen, Role of microRNA-95 in the anticancer activity of Brucein D in hepatocellular carcinoma, Eur. J. Pharmacol., 728 (2014) 141-150.

[4] O. Abdel-Rahman, Systemic therapy for hepatocellular carcinoma (HCC): from bench to bedside, J. Egypt. Natl. Cancer Inst., 25 (2013) 165-171.

[5] X. Yuan, H. Chen, X. Li, M. Dai, H. Zeng, L. Shan, Q. Sun, W. Zhang, Inhibition of protein kinase C by isojacareubin suppresses hepatocellular carcinoma metastasis and induces apoptosis in vitro and in vivo, Sci. Rep., 5 (2015).

[6] Koji, Miyahara, Kazuhiro, Nouso, Kazuhide, Yamamoto, Chemotherapy for advanced hepatocellular carcinoma in the sorafenib age, World J. Gastroenterol., 20 (2014) 4151-4159.

[7] C. Li, A.X. Jones, X. Lei, Synthesis and mode of action of oligomeric sesquiterpene lactones, Nat. Prod. Rep., 33 (2016) 602-611.

[8] X. Cheng, Q. Zeng, J. Ren, J. Qin, S. Zhang, Y. Shen, J. Zhu, F. Zhang, R. Chang, Y. Zhu, Sesquiterpene lactones from Inula falconeri, a plant endemic to the Himalayas, as potential anti-inflammatory agents, Eur. J. Med. Chem., 46 (2011) 5408-5415.

[9] Q. Jin, J.W. Lee, H. Jang, J.E. Choi, D. Lee, J.T. Hong, Y. Kim, M.K. Lee, B.Y. Hwang, Sesquiterpenes from Inula japonica with Inhibitory Effects on Nitric Oxide Production in Murine Macrophage RAW 264.7 Cells, J. Nat. Prod., (2016)

1548-1553.

[10] J.J. Qin, H.Z. Jin, J.X. Zhu, J.J. Fu, Q. Zeng, X.R. Cheng, Y. Zhu, L. Shan, S.D. Zhang, Y.X. Pan, New sesquiterpenes from Inula japonica Thunb. with their inhibitory activities against LPS-induced NO production in RAW 264.7 macrophages, Tetrahedron, 66 (2010) 9379-9388.

[11] D.R. Hwang, Y.S. Wu, C.W. Chang, T.W. Lien, W.C. Chen, U.K. Tan, J.T.A. Hsu, H.P. Hsieh, Synthesis and anti-viral activity of a series of sesquiterpene lactones and analogues in the subgenomic HCV replicon system, Biorg. Med. Chem., 14 (2006) 83-91.

[12] T.A. Mohamed, M.E.F. Hegazy, A.A.A.E. Aty, H.A. Ghabbour, M.S. Alsaid, A.A. Shahat, P.W. Paré, Antimicrobial sesquiterpene lactones from Artemisia sieberi, J. Asian Nat. Prod. Res., (2017) 1-9.

[13] A. Shakeri, E. Amini, J. Asili, M. Masullo, S. Piacente, M. Iranshahi, Screening of several biological activities induced by different sesquiterpene lactones isolated from Centaurea behen L. and Rhaponticum repens (L.) Hidalgo, Nat. Prod. Res., (2017) 1-5.

[14] T.J. Schmidt, R. Brun, G. Willuhn, S.A. Khalid, Anti-trypanosomal activity of helenalin and some structurally related sesquiterpene lactones, Planta Med., 68 (2002) 750-751.

[15] M. Ilamathi, S. Santhosh, V. Sivaramakrishnan, Artesunate as an anti-cancer agent targets Stat-3 and favorably suppresses hepatocellular carcinoma, Curr. Top Med. Chem., (2016) 2453-2463.

[16] C.Y. Liu, H.S. Chang, I.S. Chen, C.J. Chen, M.L. Hsu, S.L. Fu, Y.J. Chen, Costunolide causes mitotic arrest and enhances radiosensitivity in human hepatocellular carcinoma cells, Radiat. Oncol., 6 (2011) 1-8.

[17] D. Carlisi, A. D'Anneo, L. Angileri, M. Lauricella, S. Emanuele, A. Santulli, R. Vento, G. Tesoriere, Parthenolide sensitizes hepatocellular carcinoma cells to trail by inducing the expression of death receptors through inhibition of STAT3 activation, J. Cell Physiol., 226 (2011) 1632-1641.

[18] Y. Ren, J. Yu, K.A. Douglas, Development of anticancer agents from plant-derived sesquiterpene lactones, Curr. Med. Chem., 23 (2016) 2397-2420.

[19] M. Rozalski, U. Krajewska, M. Panczyk, M. Mirowski, B. Rozalska, T. Wasek, T. Janecki, Synthesis and biological evaluation of 4-methylideneisoxazolidin-5-ones — a new class of highly cytotoxic α-methylidene-γ-lactones, Eur. J. Med. Chem., 42 (2007) 248-255.

[20] L.M. Polo, C.M. Castro, M.C. Cruzado, C.J.G. Collino, F.D. Cuello-Carrión, D.R. Ciocca, O.S. Giordano, M. Ferrari, L.A. López, 11,13-dihydro-dehydroleucodine, a derivative of dehydroleucodine with an inactivated alkylating function conserves the anti-proliferative activity in G2 but does not cause cytotoxicity, Eur. J. Pharmacol., 556 (2007) 19-26.

[21] S.M. Kupchan, M.A. Eakin, A.M. Thomas, Tumor inhibitors. 69. Structure-cytotoxicity relations among the sesquiterpene lactones. J. Med. Chem., 14 (1971) 1147-1152.

[22] K.H. Lee, I.H. Hall, E.C. Mar, C.O. Starnes, S.A. Elgebaly, T.G. Waddell, R.I.

Hadgraft, C.G. Ruffner, I. Weidner, Sesquiterpene antitumor agents: inhibitors of cellular metabolism, Science, 196 (1977) 533-536.

[23] J.M. Woynarowski, J. Konopa, Inhibition of DNA biosynthesis in HeLa cells by cytotoxic and antitumor sesquiterpene lactones, Mol. Pharmacol., 19 (1981) 97-102.

[24] Y. Yao, D. Xia, Y. Bian, Y. Sun, F. Zhu, B. Pan, M. Niu, K. Zhao, Q. Wu, J. Qiao, C. Fu, Z. Li, K. Xu, Alantolactone induces G1 phase arrest and apoptosis of multiple myeloma cells and overcomes bortezomib resistance, Apoptosis, 20 (2015) 1122-1133.

[25] V.M. Dirsch, H. Stuppner, A.M. Vollmar, Cytotoxic sesquiterpene lactones mediate their death-inducing effect in leukemia T cells by triggering apoptosis, Planta Med., 67 (2001) 557-559.

[26] M.L. Guzman, R.M. Rossi, L. Karnischky, X. Li, D.R. Peterson, D.S. Howard, C.T. Jordan, The sesquiterpene lactone parthenolide induces apoptosis of human acute myelogenous leukemia stem and progenitor cells, Blood, 105 (2005) 4163-4169.

[27] F.F.P. Arantes, L.C.A. Barbosa, E.S. Alvarenga, A.J. Demuner, D.P. Bezerra, J.R.O. Ferreira, L.V. Costa-Lotufo, C. Pessoa, M.O. Moraes, Synthesis and cytotoxic activity of α-santonin derivatives, Eur. J. Med. Chem., 44 (2009) 3739-3745.

[28] A. Wyrębska, J. Szymański, K. Gach, J. Piekielna, J. Koszuk, T. Janecki, A. Janecka, Apoptosis-mediated cytotoxic effects of parthenolide and the new synthetic analog MZ-6 on two breast cancer cell lines, Mol. Biol. Rep., 40 (2013) 1655-1663.

[29] H. Chen, B.Y. Chen, C.T. Liu, Z. Zhao, W.H. Shao, H. Yuan, K.J. Bi, J.Y. Liu, Q.Y. Sun, W.D. Zhang, Synthesis and structure-activity relationships of guaiane-type

sesquiterpene lactone derivatives with respect to inhibiting NO production in lipopolysaccharide-induced RAW 264.7 macrophages, Eur. J. Med. Chem., 83 (2014) 307–316.

[30] H. Chen, G. Wu, S. Gao, R. Guo, Z. Zhao, H. Yuan, S. Liu, J. Wu, X. Lu, X. Yuan, Z. Yu, X. Zu, N. Xie, N. Yang, Z. Hu, Q. Sun, W. Zhang, Discovery of potent small-molecule inhibitors of ubiquitin-conjugating enzyme UbcH5c from α-santonin derivatives, J. Med. Chem., 60 (2017) 6828-6852.

Figures, Schemes and Tables

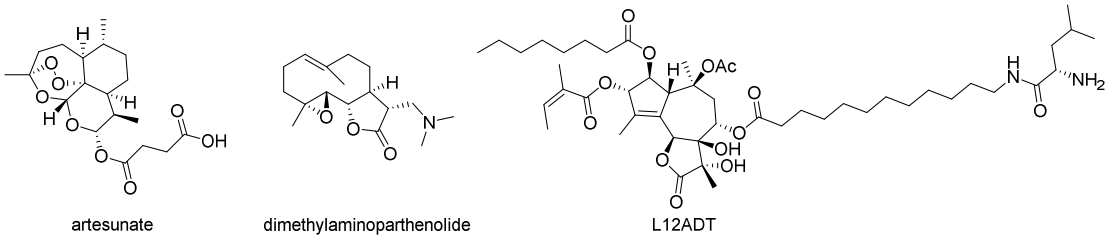

Chart 1. The chemical structures of artesunate, dimethylaminoparthenolide, and L12ADT

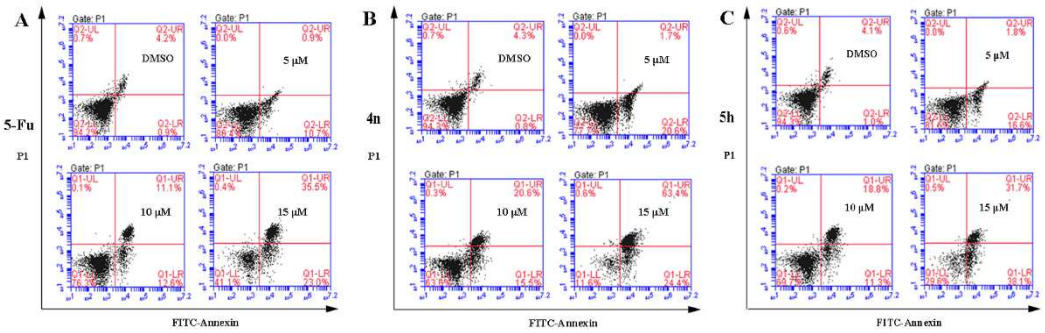

Figure 1. **5-Fu**, **4n** and **5h** induce apoptosis of QGY-7703 cells in dose-dependent manner.

QGY-7703 cells were treated with DMSO (control) or compounds **5-Fu** (**A**), **4n** (**B**) and **5h** (**C**) at dose-rising concentrations for 24 h and apoptosis was quantified using flow cytometry after staining with annexin V/PI.

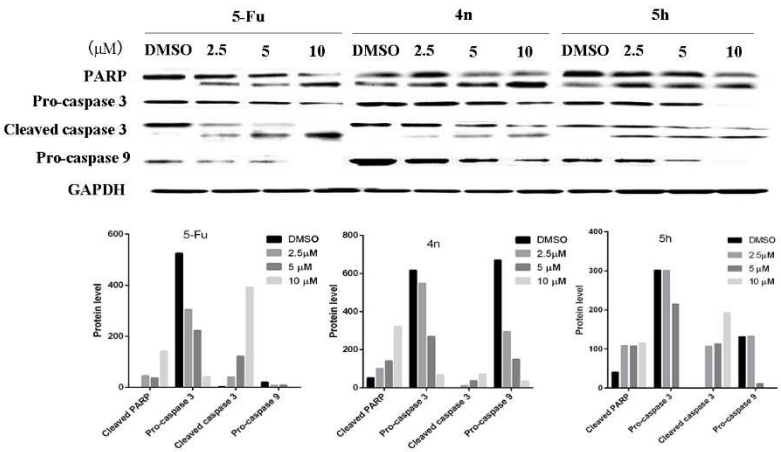

Figure 2. **5-Fu**, **4n** and **5h** induce apoptosis related proteins expression in QGY-7703 cells.

The expression of PARP, Pro-Caspase 3, Cleaved Caspase 3 and Pro-caspase was evaluated by

western blotting in 4n and 5h treated QGY-7703 cells. Quantification of data from result of western blotting were analyzed with Quantity one and data were presented in the form of grayscale value.

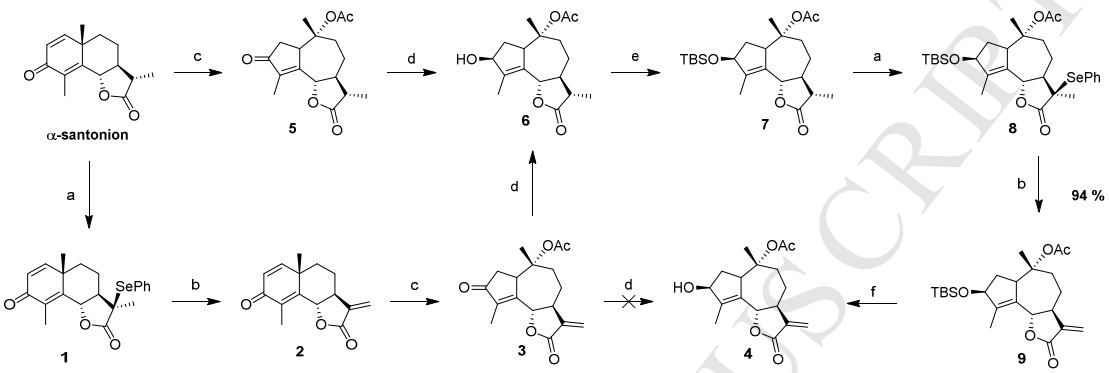

Scheme 1. Synthetic route for compound **4**.

Reagents and conditions (a) LDA/PhSeCl, THF, -78 ºC −-20 ºC, 33%; (b) 30% H_2O_2/AcOH, THF, 0 ºC−rt, 95%; (c) hυ, AcOH, 38%; (d) $NaBH_4$, MeOH, 94%; (e) TBSOTf/DIPEA, DCM, 0 ºC, 94% (f) TBAF, THF, 96%

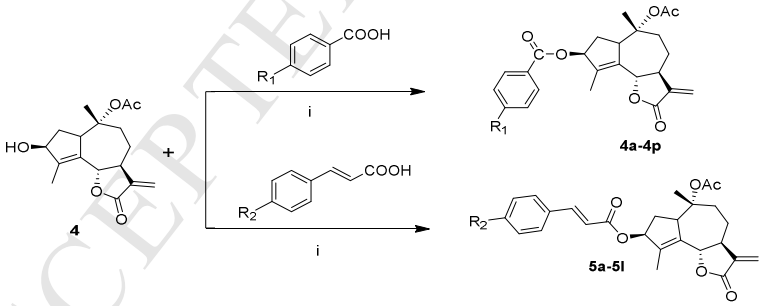

Scheme 2. Derivatives (**4a-4p** and **5a-5l**) of compound **4**.

Reagents and conditions: (i) EDCI, DMAP, DCM, room temperature, overnight, 70-98%.

Table 1. Inhibition rates of compounds **4**, **4a-4p** and **5a-5l** against the HepG-2 cell line (10 μM)

Compd.	R_1	Inhibition rate (%)	Compd.	R_2	Inhibition rate (%)

4		32.02	**5a**	-H	56.11
4a	-H	68.47	**5b**	-Me	72.03
4b	-Me	58.47	**5c**	-SMe	36.24
4c	-Et	42.33	**5d**	-OMe	61.14
4d	-Pr-n	62.47	**5e**	-OEt	49.75
4e	-Bu-n	67.53	**5f**	-OPr-n	47.78
4f	-amyl-n	58.08	**5g**	-F	67.53
4g	-Pr-i	37.86	**5h**	-Cl	62.92
4h	-Bu-t	64.41	**5i**	-Br	61.39
4i	-OMe	53.03	**5j**	-NC	48.53
4j	$-OCF_3$	69.25	**5k**	$-CF_3$	71.14
4k	$-CF_3$	72.42	**5l**	$-NO_2$	42.67
4l	-CN	62.58	**5-Fu**		50.58
4m	-F	78.61			
4n	-Cl	72.69			
4o	-Br	71.06			
4p	-I	63.11			

Table 2. Antiproliferative activities of target compounds against human HCC cells and hepatocytes.

Compd.	**IC_{50} (μM)**			
	HepG-2	QGY-7703	SMMC-7721	QSG-7701
4a	7.99	12.96	5.99	>100
4b	8.52	12.21	6.49	>100
4d	10.11	8.33	6.52	34.27
4e	10.32	7.20	7.46	45.06
4f	10.77	7.19	18.70	38.48
4h	11.14	5.13	9.37	48.49
4i	12.21	22.26	8.93	>100
4j	7.54	11.30	6.10	36.81
4k	5.63	5.64	5.49	41.11
4l	9.14	22.80	6.70	>100
4m	6.20	6.78	4.97	39.04
4n	7.10	10.11	4.24	46.91
4o	7.41	13.70	6.54	51.91
4p	7.57	9.00	4.18	36.48
5a	16.22	18.80	6.43	>100
5b	8.67	10.60	5.06	>100

5d	12.11	11.78	5.41	>100
5g	9.98	12.20	5.80	>100
5h	7.51	3.06	4.08	>100
5i	11.65	8.91	6.09	91.28
5k	6.79	12.71	6.12	43.26
5-Fu	15.74	14.20	12.47	6.92

(a) A series of α-santonin-derived compounds were synthesized.

(b) The structure-activity relationships were preliminary investigated.

(c) These derivatives exhibited activities against HCC cells by up-regulate apoptotic-associated proteins.

(d) Derivative **5h** had better selectivity against the tumor cells over normal hepatic cell line than 5-Fu.